Polymer Bulletin (2023) 80:3055–3083
https://doi.org/10.1007/s00289-022-04181-7

ORIGINAL PAPER

A DFT study of vibrational spectra of 5-chlorouracil with molecular structure, HOMO–LUMO, MEPs/ESPs and thermodynamic properties

J. S. Singh[1] · Mohd. Shahid Khan[1] · Saeed Uddin[1]

Received: 20 October 2021 / Revised: 12 February 2022 / Accepted: 6 March 2022 /
Published online: 31 March 2022

Abstract

The density functional theory calculation has been carried out for the analysis of 5-chlorouracil using DFT/Gaussian 09 with GAR2PED. Recorded experimental spectra for Raman and IR of 5-chlorouracil have been analyzed all fundamental vibrational modes using the outcome results of DFT at 6-311++G** of Gaussian 09 calculations and the GaussView 5.09. To help the analysis of vibrational modes, GAR2PED program has been used in the calculation of PEDs. The charge transfer properties of 5-chlorouracil have been analyzed using HOMO and LUMO level energy analysis. HOMO and LUMO energy gap study supports the charge transfer possibility in molecule. These have been made to study for reactivity and stability of *heterocyclic molecules* for the analysis of antiviral drugs against the new corona virus: COVID-19. Here, the *smaller energy gap* of 5-chlorouracil is more responsible for charge transfer interaction in the *heterocyclic drug molecules* and a reason of more bioactivity. The electron density mapping within molecular electrostatic potential plot and electrostatic potential plotting within iso-surface plot have been evaluated the charge distribution concept in the molecule as the nucleophilic reactions and electrophilic sites. These computations have been used to produce the molecular charges, structure and thermodynamic functions of biomolecule. This study has been made to all internal modes of chloro group substituent at pyrimidine ring of C_5 atom. The splitting of frequencies has arisen in the two species for the normal distribution modes.

✉ J. S. Singh
jssaec@rediffmail.com; jssaec@gmail.com

[1] Department of Physics, Jamia Millia Islamia (Central University), New Delhi 110025, India

Graphical abstract

A molecular analysis and vibrational spectra of 5-chlorouracil

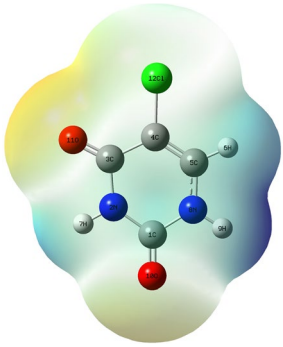

MEP Plot of 5-chlorouracil

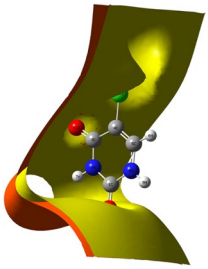

Iso-Surface plot of ESP Contour Map of 5-chlorouracil

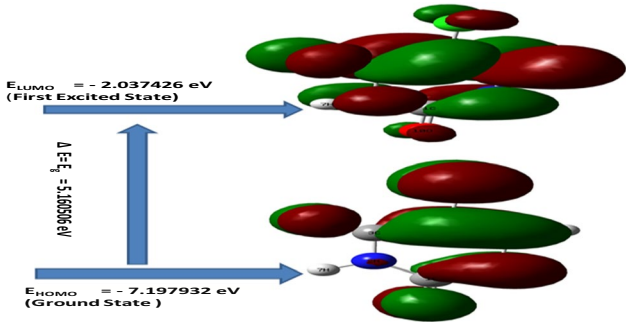

Pictorial Separation of Electronic Energy Levels with frontier MOs of 5-chlorouracil

Keywords DFT/G-09 · Vibrational spectra · HOMO–LUMO · MEPs/ESPs · Thermodynamics

Introduction

Heterocycle-shaped 5-chlorouracil is the aromatic organic biomolecule. The pyrimidine-based parent molecule, uracil, is the main constituent of ribonucleic acid (RNA), but it is exchanged by 5-methyl-uracil (thymine) for deoxyribonucleic acid (DNA). The halo-uracils are used as antitumor agents. The derivatives of uracil have an important role in their chemical/physical as well as optical behavior in vivo activity, bioactivity and pharmacological activities. Therefore, the widely used derivatives in medical society are 5-fluoro-uracil as anticancer drug, 5-iodo-uracil and 5-trifluoro-methyl-uracil in antiviral activities. Hence, their derivatives are wide discussing for their optical and biological actives [1–3] for anticarcinogenic and anti-HIV viruses drugs [4–8], as well as in the analysis of antiviral drugs against the new corona virus: COVID-19. The halogenated pyrimidines are normally used in anticarcinogenic drugs as for the treatment of tumor as well as the colorectal cancer [4, 5]. Therefore, their derivatives have been tested as drugs for anti-HIV as well as the antitumor [6, 8]. This article is depending upon the study of vibrational modes of chloro group on the uracil's ring. The study of 5-substituted uracils [9–23] has been done through so many researchers, but here it is needed for a more study at place of C_5 atom on ring of uracil for a further study.

So, it is made the calculations of 5-chlorouracil for optimized geometries, atomic charges on atomic sites and all fundamental modes applying the basis set 6-311++G** of Gaussian 09 [24]. All of fundamental modes have been optimized with the help of calculated modes and are obtained the related parameters. Here, it is also investigated the reactivity of 5-chlorouracil molecule using HOMO–LUMO analysis for charge density transfer, orbital energies and electrostatic potential analysis.

Material and methods

Experimental

Without any further purification, a spectral grade of 5-chlorouracil crystalline powder of Aldrich chem. Co. (USA) was used in spectra recording of IR and Raman. All spectra have been recorded at normal room temp (23 °C) in solid phase for spectroscopic analysis. Infrared spectrum as reproduced in Fig. 1 (a) has been recorded at normal temperature (23 °C) in the range of 400–4000 cm^{-1} by the FTIR (Model-5300) spectrophotometer. Raman spectra as shown in Fig. 2 (a) were recorded at same temperature at the Raman spectrophotometer (model Spex-1877) between the 200 and 4000 cm^{-1} with the help of an excitation source of Argon ion (Ar^{+}) laser line of 4880 A^{0}. The resolution of spectra of IR and Raman was better than the 2 cm^{-1} and an accuracy of 2 cm^{-1}.

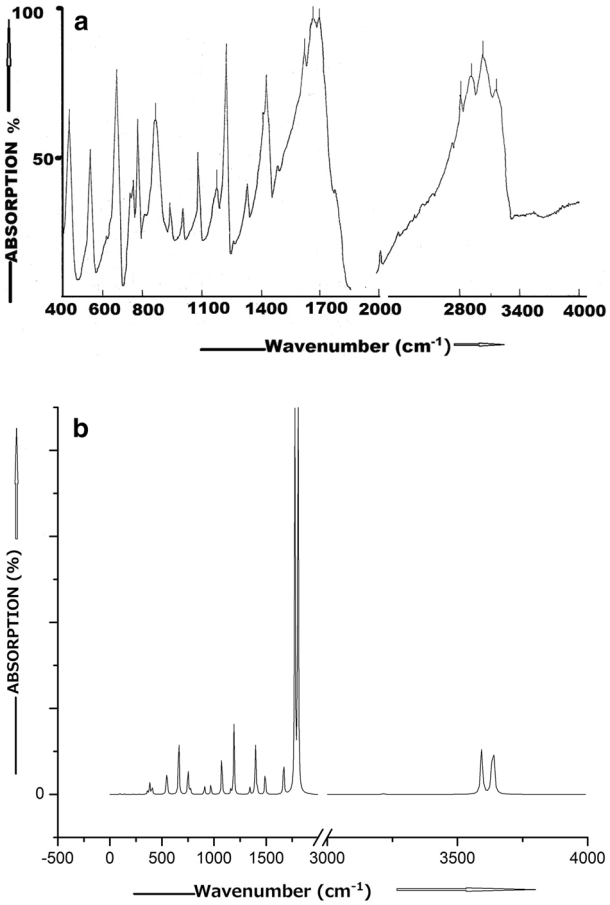

Fig. 1 **a** IR spectrum of 5-chlorouracil, **b** calculated IR spectrum of 5-chlorouracil

Theoretical

In study of 5-chlorouracil, it was carried out the DFT (SCF) calculation using Gaussian 09 program [24] and the optimization of geometry was done at B3LYP/6-311++G** with minimum energies for all geometrical parameters. All of the evaluated fundamental frequencies have been optimized with the help of visualization program GaussView [25] of G-09 [24] and evaluated PEDs from GAR2PED [26]. Here, it is calculated the bond angles, lengths with infrared intensities (Fig. 1-b) as well as the depolarization ratio of Raman peaks with Raman scattering activities (Fig. 2-b) of 5-chlorouracil. This study has also evaluated the thermodynamic functions and other properties of the biomolecule as given in Fig. 3 (a, b). In this study, the visualized demonstrations of molecular electrostatic potentials (MEPs) show electrophilic/nucleophilic reactive location for a justification of theoretical biological activities with H bonding interactions. HOMO and LUMO energy gap is

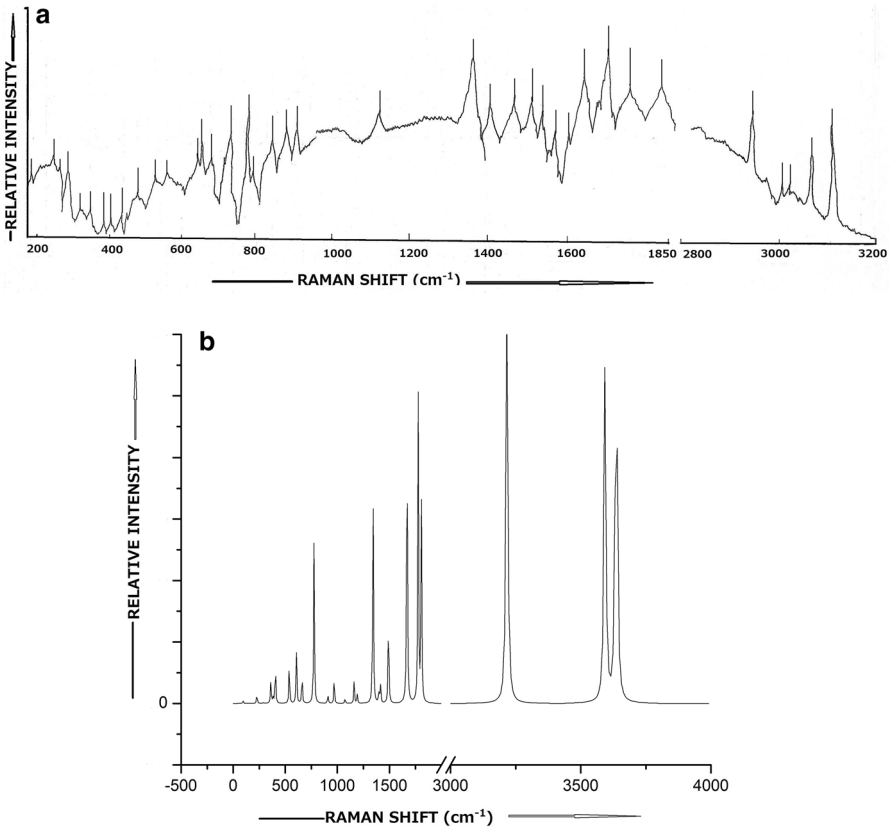

Fig. 2 **a** Raman spectrum of 5-chlorouracil, **b** calculated Raman spectrum of 5-chlorouracil

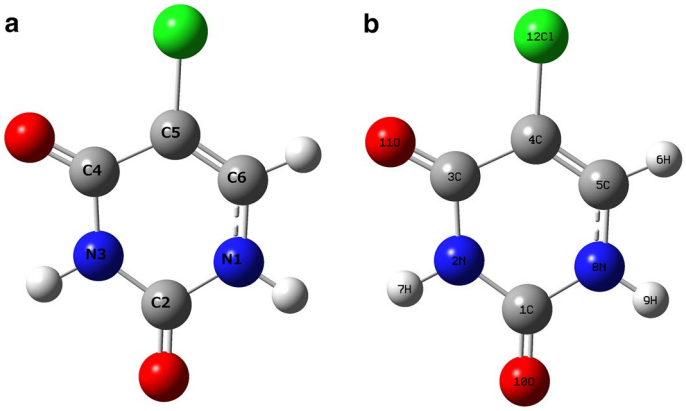

Fig. 3 **a** Numbering for nomenclature of pyrimidine ring of 5-chlorouracil, **b** numbering scheme for optimization of 5-chlorouracil

optimized with the help of Gaussian 09 program [24] to study of the charge transfer possibility within molecule.

Results with discussion

Molecular charges

The molecular charge explanation has been based on Mulliken charges and it can be derived with the help of the suitable computed atomic polar tensor charges. Cioslowski has defined the atomic charges by atomic polar tensor (APT) invariants [27]. The molecular charges can be optimized on different basis set of Gaussian 09 program [24]. These optimizations satisfy the neutrality of molecule, and they are related to the observed results of IR intensities. Their properties contributed to the success of molecular charges and help to understand generalized atomic polar tensor charges [28–30].

APT charges: These charges have been represented a charge–charge flux model as sum of charge tensor and charge flux [31]. The partial atomic polar charges arise all over molecular surface that these represent all chemical properties [32, 33]. Atomic labeling diagram of 5-chlorouracil is given in Fig. 3 (b). APT charges at atoms of 5-chlorouracil molecule have been computed applying the 6-311++G** basic level [24]; these are summarized in Table 1. In Table 1, the comparison of higher atomic electronegativity has been made with other −ve charge atomic positions. Atomic polar tensor charges of 5-chlorouracil are explained with respect of atoms as follows. In pyrimidine ring, the C_4 atom [as at C_5 on ring of 5-chlorouracil as shown in Fig. 3 (a)] atom has the negative ATP charge − 0.036774 a.u., but the rest of three carbons C_1, C_3 and C_5 have +ve charge, respectively, as 1.353079, 1.111933 and 0.439128 a.u. and only C_4 shows the reactant property than the other carbon atoms. The oxygen atoms O_{10} and O_{11} bear −ve APT charge -0.918364 and − 0.793447 a.u.

Table 1 Optimized atomic polar tensor[$] and Mulliken charges[$] at atomic sites of 5-chlorouracil

No	Atoms[#]	ATP charges[$]	Mulliken charges[$]
1	C_1	1.353079	0.332236
2	N_2	− 0.728977	− 0.406186
3	C_3	1.111933	− 0.088012
4	C_4	− 0.036774	0.317438
5	C_5	0.439128	− 0.457703
6	H_6	0.081201	0.198048
7	H_7	0.224456	0.365097
8	N_8	− 0.752779	− 0.361195
9	H_9	0.250381	0.344104
10	O_{10}	− 0.918364	− 0.333142
11	O_{11}	− 0.793447	− 0.269039
12	Cl_{12}	− 0.229838	0.358353

[#]The numbering of atom is shown in Fig. 3 (b)

[$]unit of e

at respective atoms. Similarly nitrogen atoms, N_2 and N_8 show APT charge negative − 0.728977 and − 0.752779 a.u. at respective atoms of 5-chlorouracil. Because of the larger electronegativity, all atoms of oxygen and nitrogen bear negative APT charges. Here, the three atoms of hydrogen (H_6, H_7, H_9) on pyrimidine ring of 5-chlorouracil bear + ve APT charge 0.081201, 0.224456 and 0.250381 a.u, respectively. In addition, Cl_{12} atom bears negative APT charge − 0.229838a.u. Here, it could be found that the C_4 atom is having negative charge in all of C_1, C_3, C_4 and C_5 carbon atoms. So for, it is noticed that all of hydrogen atoms (H_6, H_7, H_9) on the ring which are attached direct to the atoms of nitrogen and bear + ve APT charges.

Mulliken atomic charges: Here, this charge calculation has an application of DFT optimization for the geometry of molecule, electronic structure, atomic charges and dipole moment with other more properties [31]. Mulliken atomic charges [31] play a useful application in the quantum chemical calculation that this depends on the basis set. In the molecule, the partial charges come out at surface which shows all chemical properties [32, 33]. These charges at atomic places, as given in Fig. 3 (b), of 5-chlorouracil are optimized at level 6-311++G** [24], and they are summarized in Table 1. Here, this could be found that the C_1 and C_4 of pyrimidine ring have the + ve charges, respectively, as 0.332236 and 0.317438 a.u., except the C_3 and C_5 atom in ring bear the −ve charges, respectively, as −0.088012 and −0.457703 a.u. due to chloro atom. The two O_{10} and O_{11} have the −ve charges as −0.333142 and −0.269039 a.u., respectively. Similarly, nitrogen atoms N_2 and N_8 of 5-chlorouracil have the Mulliken charges –ve as −0.406186 and −0.361195 a.u. for corresponding atom. So far, all of the nitrogen and oxygen have the high electronegativity. The three hydrogen (H_6, H_7 and H_9) atoms on pyrimidine ring of 5-chlorouracil bear + ve charges as 0.198048, 0.365097 and 0.344104 a.u. to the respective hydrogen. On ring, the atom Cl_{12} has the + ve Mulliken atomic charge 0.358353 a.u., and this is noticed that the Cl_{12} atom has the -ve charge as the case of atomic polar tensor (APT) charges.

Molecular structural geometry

Atomic numbering scheme and optimized molecular structural geometry corresponding to 5-chlorouracil biomolecule is given in Fig. 3(b). The optimizations of geometrical parameters of 5-chlorouracil are summarized in Table 2. These geometrical parameters suggest that the chloro group is replaced on the ring of H atom at C_4 atom [as on C_5 ring atom of 5-chlorouracil as shown in Fig. 3(a)] on uracil pyrimidine ring. In pyriminide ring, the optimized structures of 5-chlorouracil show that all bonds of the ring bear the partial double bond character. As given in Table 2, four C-N bonds of pyrimidine ring of 5-chlorouracil are having the lengths in the descending order of (N_2–C_3, N_8–C_1, N_2–C_1, C_5–N_8), are mostly similar in their magnitudes to each molecules lie between bond length ~ 1.41 Å and ~ 1.37 Å, and are lying in a plane of pyriminide ring. In addition, the rest two bonds of the ring, C_3–C_4 and C_4=C_5 bonds have been had in the order of (C_3–C_4) > (C_4=C_5) bearing the values ~ 1.47 Å and ~ 1.35 Å. And the C_4–Cl_{12} bond holds the length 1.734 Å.

Table 2 Optimization of structural parameters of 5-chlorouracil

Definition[#]	5-chlorouracil
Bond lengths (r) in $\overset{0}{A}$	
$r(N_2–C_1)$	1.3852
$r(N_8–C_1)$	1.3916
$r(C_1–O_{10})$	1.2111
$r(N_2–C_3)$	1.4093
$r(N_2–H_7)$	1.0129
$r(C_3–C_4)$	1.4692
$r(C_3–O_{11})$	1.2098
$r(C_4=C_5)$	1.3484
$r(C_4–Cl_{12})$	1.734
$r(C_5–H_6)$	1.0817
$r(C_5–N_8)$	1.3745
$r(N_8–H_9)$	1.0092
Bond angles (α) in degree (°)	
$\alpha(N_2–C_1–N_8)$	112.6902
$\alpha(N_2–C_1–O_{10})$	124.2475
$\alpha(N_8–C_1–O_{10})$	123.0621
$\alpha(C_1–N_2–C_3)$	128.8584
$\alpha(C_1–N_2–H_7)$	115.5275
$\alpha(C_3–N_2–H_7)$	115.614
$\alpha(N_2–C_3–C_4)$	112.6205
$\alpha(N_2–C_3–O_{11})$	120.9095
$\alpha(C_4–C_3–O_{11})$	126.47
$\alpha(C_3–C_4–C_5)$	120.3401
$\alpha(C_3–C_4–Cl_{12})$	118.1483
$\alpha(C_5–C_4–Cl_{12})$	121.5116
$\alpha(C_4–C_5–H_6)$	122.2265
$\alpha(C_4–C_5–N_8)$	121.6007
$\alpha(H_6–C_5–N_8)$	116.1728
$\alpha(C_1–N_8–C_5)$	123.89
$\alpha(C_1–N_8–H_9)$	115.4067
$\alpha(C_5–N_8–H_9)$	120.7033
Dihedral angles (δ) in degree (°)	
$\delta(N_8–C_1–N_2–C_3)$	− 0.16
$\delta(N_8–C_1–N_2–H_7)$	− 179.97
$\delta(O_{10}–C_1–N_2–C_3)$	180.01
$\delta(O_{10}–C_1–N_2–H_7)$	0.13
$\delta(N_2–C_1–N_8–C_5)$	0.12
$\delta(N_2–C_1–N_8–H_9)$	180.04
$\delta(O_{10}–C_1–N_8–C_5)$	− 180.03
$\delta(O_{10}\text{-}C_1\text{-}N_8\text{-}H_9)$	− 0.11
$\delta(C_1–N_2–C_3–C_4)$	0.11
$\delta(C_1–N_2–C_3–O_{11})$	− 180.14

Table 2 (continued)

Definition[#]	5-chlorouracil
$\delta(H_7–N_2–C_3–C_4)$	180.02
$\delta(H_7–N_2–C_3–O_{11})$	− 0.00
$\delta(N_2–C_3–C_4–C_5)$	− 0.01
$\delta(N_2–C_3–C_4–Cl_{12})$	180.03
$\delta(O_{11}–C_3–C_4–C_5)$	180.04
$\delta(O_{11}–C_3–C_4–Cl_{12})$	− 0.0 5
$\delta(C_3–C_4–C_5–H_6)$	− 180.02
$\delta(C_3–C_4–C_5–N_8)$	− 0.02
$\delta(Cl_{12}–C_4–C_5–H_6)$	− 0.00
$\delta(Cl_{12}–C_4–C_5–N_8)$	− 180.00
$\delta(C_4–C_5–N_8–C_1)$	− 0.04
$\delta(C_4–C_5–N_8–H_9)$	− 179.96
$\delta(H_6–C_5–N_8–C_1)$	179.96
$\delta(H_6–C_5–N_8–H_9)$	0.04

[#]The numbering scheme is shown in Fig. 3 (b)

So in the notice, these angles of ring C-N–C, C–C–N and C–C–C are unequal, and hold as smallest $\alpha(N_2–C_3–C_4)$, angle value 112.69^0, largest α $(C_1–N_2–C_3)$ and third angle value of 128.86^0 in molecule, as well as in the twenty-four dihedral angles are $\sim 0^0 \pm 0.1$ or $\sim 180^0 \pm 1.0$ that show for all of 12 atoms of 5-chlorouracil, C_1, N_2, C_3, C_4, C_5, N_8, O_{10}, O_{11}, H_6, H_7, H_9 and Cl_{12} are laying in a same plane. Due to the above results, here this predicts that almost of structural parameters are same, and all of atoms in ring of pyriminide to biomolecule lie in a same plane.

Vibrational assignments

Recently, the biological significance of the biomolecules and derivatives is more discussing for the biological activities [1–3]. Due to spectroscopic investigation, vibrational study of 5-halogenated uracil with substituent of chloro group is assigned for the *fifth* position site of ring. Here a detailed study of 5-chlorouracil at *fifth* position (C_5) of ring with due respect to mass and electronegativity in order of hydrogen < chlorine atom has been carried out and it is discussed with an experimental and theoretical study on the 5-chlorouracil molecule in the light of the above properties. The vibrational study of the pyrimidine ring and its derivatives has similarity with benzene ring and its derivatives. This assignment is made especially for planarity and non-planarity of the internal mode at C_5 of uracil for substituent of atom which might cause the modes splitting and that this could be happened for the reason of mass and electronegativity of the substitution at C_4 ring atom [as at C_5 atom on pyrimidine ring of 5-chlorouracil as shown in Fig. 3 (a)]. The fundamental frequencies have been reported with the help of computed frequencies and through the GaussView visualization program [25] of G-09 [24], and PEDs have been calculated by GAR2PED program [26]. Thus, 5-chlorouracil has 12 atoms with the 30 fundamental modes bearing C_s symmetry, and all of the fundamental frequencies are

expected to be appeared in Raman and IR spectra. Optimized computation is carried out for the vibrational modes, and their infrared intensities (Fig. 1b), Raman depolarization ratio and scattering activities (Fig. 2b) are summarized in Table 3. The symmetric vibrational calculation as well as observation of all normal frequencies of 5-chlorouracil is summarized in Table 3 along with PEDs as shown in Fig. 3(b) and their results have been discussed as follows.

C–Cl (three modes): Here for stretching, the ν (C–Cl) mode of chlorine bond has appeared at upper frequencies region compare to aromatic compound group. In assignment of 5-chlorouracil, ν (C–Cl) vibration was reported with ~ 1275 cm^{-1} [16]. Now, ν (C_4–Cl_{12}) vibration has been calculated at 660 cm^{-1}, but it has been recorded the IR at 670 cm^{-1} and Raman at 661 cm^{-1} showing the strong intensity as well as largely mixing within the other modes of pyrimidine ring, which is much lower than the reported work [16]. In-plane, the β (C–Cl) mode is reported between the 300 and 250 cm^{-1} to ref. [16] and to be nearly similar to the region. Hence, this region is reported nearly or below at ~ 300 cm^{-1}. The optimized mode for β (C_4–Cl_{12}) has been found at 227 $cm^{-1}$and at 260 cm^{-1} in Raman, but it is quite below for the reason of mass and electronegativity of chloro group. And for out-of-plane vibration, the γ(C_4 –Cl_{12}) is optimized at 286 cm^{-1} and recorded Raman band at 290 cm^{-1}, and it has mixed up with the H bonding. So far, this could be found that the out-of-plane ring deformation and in-plane bending modes are correctly assigned to be possible with the PEDs in such lower region of reported work [16].

C–H (three modes): For the ν(C–H) fundamentals, these are known as the strong characteristic vibrational modes in biomolecules [3] and appear between the range 3000 and 3300 cm^{-1}[19]. Here the modes in-plane, these two modes ν(C_5–H_6) and β (C_5–H_6) have been optimized at 3217 and 1343 cm^{-1} and these have been recorded at 3060 and 1340 cm^{-1} in IR and at 3060 and 1346 cm^{-1} in the Raman band, respectively, with strong intensities; here, one of the ν(C_5–H_6) modes is a characteristic band as with a strong appearance in PEDs. In non-planar modes, the γ (C_5–H_6) vibration are optimized at 910 cm^{-1} with recorded in IR at 880 cm^{-1} and Raman peak at 900 cm^{-1}. So for, it is happened that ν(C–H) vibration has been found to be the one of more sensitive with a reason of the Ar matrix isolation of molecule than the solid molecular phase [19]. Hence, it is found that these above assignments have a parallel agreement to the works [9–21].

N–H (six modes): Similarly, the stretching fundamentals of C–H, the ν (N–H) vibrations are found as other strong characteristic bands in biomolecules [3] and which appears between the ranges 3200 and 3600 cm^{-1}, but the problems in experimental and theoretical values have been arisen with modes of N–H for an involvement of the contributions of few other normal modes [19]. So for in-plane modes, the ν (N_8–H_9) and ν (N_2–H_7) modes have been optimized at 3636 and 3593 cm^{-1}, but these have been recorded at 3180 and 3160 cm^{-1} in the IR and at – and 3158 cm^{-1} in the Raman peaks and these modes intensities have been found with strong value as characteristic band in PEDs. In-plane, the β (N_8–H_9) and β (N_2–H_7) modes have been computed at 1491 and 1414 cm^{-1} and these are recorded at 1496 and 1425 cm^{-1} in

Table 3 Vibrational frequencies* of 5-chlorouracil

S. No	Distribution of vibrational modes	Exp. recorded spectra (cm^{-1})		Theoretically calculated frequencies at the DFT/B3LYP/6–311 + + G**-09 level	PEDs	Assignments[$] for the characterizations of modes	Species	
		Figure 1(a)	Figure 2(a)					
		IR	Raman	5-chlorouracil	5-chlorouracil		In-plane	Out-of-plane
1	30 vibrational modes as uracil skeleton = (21 a' + 9 a")	3180 (m)	—	3636 (120.5,109.6) 0.19	$\nu(N_8–H_9)$ (100)	ν ($N_8–H_9$)	**a'**	
2		3160 (s)	3158 (s)	3593 (77.65, 80.91) 0.23	ν($N_2–H_7$) (89) + α ($C_1–C_2–C_3$) (6) -α ($C_2–C_3–C_4$) (4)	ν ($N_2–H_7$)	a'	
3		3060 (m)	3060 (s)	3217 (01.40, 85.33) 0.31	ν ($C_5–H_6$) (88) + α ($C_2–C_3–C_4$)(8)	ν ($C_5–H_6$)	a'	
4		1792 (vs)	1810 (s)	1806 (765.4, 34.16) 0.17	α ($C_2–C_3–C_4$) (43) + ν $C_1=O_{10}$)(26) -α ($C_1–C_2–C_3$) (12)—$\nu(N_2–C_1)$ (7) + α ($C_2–C_3–C_4$) (5)	ν ($C_1=O_{10}$)	a'	
5		1772 (vs)	1772 (vs)	1776 (632.1, 45.98) 0.33	α ($C_1–C_2–C_3$) (45.)—α ($C_2–C_3–C_4$) (29)—$\nu(C_3=O_{11})$ (17)	ν ($C_3=O_{11}$)	a'	

Table 3 (continued)

S. No	Distribution of vibrational modes	Exp. recorded spectra (cm^{-1})		Theoretically calculated frequencies at the DFT/B3LYP/6–311 + + G**-09 level	PEDs	Assignments[$] for the characterizations of modes	Species	
		Figure 1(a)	Figure 2(a)					
		IR	Raman	5-chlorouracil	5-chlorouracil		In-plane	Out-of-plane
6		1666 (s)	1665 (vs)	1668 (79.37, 52.05) 0.13	$\beta(C_5–H_6)$ (53)—$\nu(C_4=C_5)$ (27) + α ($C_1–C_2–C_3$) (14)	ν($C_4=C_5$) ring	a’	
7		1496 (ms)	1496 (s)	1491 (51.41, 14.69) 0.50	$\beta(N_8–H_9)$ (34)—$\nu(N_8–C_5)$ (20)—α ($C_1–C_2–C_3$) (17)—$\beta(C_5–H_6)$ (8) + ν $C_1=O_{10}$) (7)—$\nu(N_2–C_3)$ (5) + ν ($N_8–C_1$) (4)	$\beta(N_8–H_9)$	a’	
8		1420 (s)	1425 (ms)	1414 (12.52, 03.10) 0.74	$\beta(C_5–H_6)$ (43)—$\beta(N_2$-$H_7)$ **(27)** + $\nu(N_2–C_1)$ (9) + $\alpha(C_2–C_3–C_4)$ (7)—ν ($C_3=O_{11}$) (3)	$\beta(N_2–H_7)$	a’	

Table 3 (continued)

S. No	Distribution of vibrational modes	Exp. recorded spectra (cm^{-1})		Theoretically calculated frequencies at the DFT/B3LYP/6–311 + + G**-09 level	PEDs	Assignments[$] for the characterizations of modes	Species	
		Figure 1(a)	Figure 2(a)					
		IR	Raman	5-chlorouracil	5-chlorouracil		In-plane	Out-of-plane
9		1402 (s)	1400 (s)	1398 (109.9, 01.64) 0.74	α (C_2–C_3–C_4) (27.) + β(C_5-H_6) (17) -α(C_1–C_2–C_3) (16) + ν(N_2– C_1) (9) + ν (N_2–C_3) (7)—ν(C_3–C_4) (4)—ν(N_8 –C_1) (4) + β(N_8–H_9) (4)	ν (ring)	a’	
10		1340 (s)	1346 (vs)	1343 (12.53, 29.20) 0.29	β(C_5-H_6) (62) + α (C_1–C_2–C_3) (15) + α(C_2–C_3–C_4) (11)—α(C_2–C_3–C_4) (6)	β (C_5-H_6)	a’	
11		1080 (s)	1050 (sh)	1075 (80.96, 00.66) 0.61	15 α (C_1–C_2–C_3) (58.) -13 α (C_2–C_3–C_4) (33.)	α (ring) Trigonal bending	a’	

Table 3 (continued)

S. No	Distribution of vibrational modes	Exp. recorded spectra (cm^{-1})		Theoretically calculated frequencies at the DFT/B3LYP/6–311 + + G**-09 level	PEDs	Assignments[$] for the characterizations of modes	Species	
		Figure 1(a)	Figure 2(a)					
		IR	Raman	5-chlorouracil	5-chlorouracil		In-plane	Out-of-plane
12		1190 (vs)	—	1191 (126.3, 01.44) 0.54	$\beta(C_5\text{-}H_6)$ (56) + α (C_2–C_3–C_4) (15) + $\nu(N_2$– $C_1)$ (10)—α (C_2–C_3–C_4) (6)—ν (N_2 –C_3) (4)	ν (ring)	a’	
13		1170 (ms)	1160 (ms)	1161 (11.44, 02.83) 0.68	ν (N_2 –C_3) (23) + α (C_2–C_3–C_4)(18) -ν(N_8 –C_5) (12)—$\nu(N_2$–C_1)(11)—α (C_2–C_3–C_4) (11)—$\beta(C_5\text{-}H_6)$ (7)—$\nu(C_3$–$C_4)$ (4) + $\nu(N_8$ –$C_1)$ (4)	ν (ring) Kekule	a’	
14		960 (ms)	930 (ms)	970 (19.30, 03.17) 0.57	α (C_1–C_2–C_3) (55) + $\beta(C_5$–$H_6)$ (25)—ν (N_8 –C_1)(6)—$\nu(N_2$–C_1) (4)	ν (ring)	a’	

Table 3 (continued)

S. No	Distribution of vibrational modes	Exp. recorded spectra (cm^{-1})		Theoretically calculated frequencies at the DFT/B3LYP/6–311 + + G**-09 level	PEDs	Assignments[$] for the characterizations of modes	Species	
		Figure 1(a)	Figure 2(a)					
		IR	Raman	5-chlorouracil	5-chlorouracil		In-plane	Out-of-plane
15		880 (vs	900 (ms)	910 (18.31, 01.18) 0.75	$\gamma(C_5–H_6)(50)—\delta(C_1–C_2–C_3\text{-}C_4)(35)+\delta(C_2–C_3–C_4–C_5)(9)—\delta(C_3–C_4–C_5–H_6)(7)$	γ (C_5-H_6)		a”
16		775 (vs)	776 (vs)	776 (07.90, 19.01) 0.07	$\alpha(C_1–C_2–C_3)(55)—\alpha(C_2–C_3–C_4)(18)+\nu(C_3–C_4)(6)+\nu(N_2–C_1)(5)+\nu(N_8–C_1)(5)+\nu(N_2–C_3)(4)$	ν(ring) breathing	a’	
17		760 (s)	760 (s)	764 (08.55, 00.31) 0.75	$\delta(C_1–C_2–C_3–C_4)$ (37.)—$\delta(C_3–C_4–C_5–H_6)(31)—\gamma(C_3=O_{11})(18)+\gamma(C_4–Cl_{12})(5)—\gamma(C_5–H_6)(4)$	γ (C_3=O_{11})		a”

Table 3 (continued)

S. No	Distribution of vibrational modes	Exp. recorded spectra (cm^{-1})		Theoretically calculated frequencies at the DFT/B3LYP/6–311 + + G**-09 level	PEDs	Assignments[$] for the characterizations of modes	Species	
		Figure 1(a)	Figure 2(a)					
		IR	Raman	5-chlorouracil	5-chlorouracil		In-plane	Out-of-plane
18		750 (s)	750 (sh)	749 (55.07, 00.02) 0.75	δ (C_3–C_4–C_5–H_6) (34)—γ (C_1 = O_{10}) (28)—δ (C_1–C_2–C_3–C_4) (22)—γ (N_2–H_7) (7) + γ (C_5–H_6) (5)	γ (C_1=O_{10})		a”
19		670 (vs)	670 (ms)	661 (82.71, 01.04) 0.75	γ(N_2–H_7)(62)—α (C_2–C_3–C_4) (12)—α(C_2–C_3–C_4) (9) -δ(C_2–C_3–C_4–C_5) (4)	γ(N_2–H_7)		a”
20		670 (s)	661 (s)	660 (47.30, 02.78) 0.06	α (C_2–C_3–C_4) (47) + α(C_2–C_3–C_4) (36) + ν(C_4 –Cl_{12}) (6) + ν(C_3–C_4) (4)	ν (C_5 –Cl_{12})	a’	

Table 3 (continued)

S. No	Distribution of vibrational modes	Exp. recorded spectra (cm^{-1})		Theoretically calculated frequencies at the DFT/B3LYP/6–311 + + G**-09 level	PEDs	Assignments[$] for the characterizations of modes	Species	
		Figure 1(a)	Figure 2(a)					
		IR	Raman	5-chlorouracil	5-chlorouracil		In-plane	Out-of-plane
21		610 (ms)	630 (s)	607 (00.16, 06.28) 0.43	α (C_1–C_2–C_3) (52)—α (C_2–C_3–C_4) (26) + β(C_1 = O_{10}) (6)—β (C_3=O_{11}) (6)	β (C_1=O_{10})	a’	
22		550 (vs)	555 (m)	548 (54.12, 00.11) 0.75	γ(N_8–H_9) (88)—γ(N_2–H_7) (7)—γ(C_3=O_{11}) (3)	γ(N_8–H_9)		a”
23		540 (sh)	535 (ms)	538 (08.45, 04.62) 0.27	13 α (C_2–C_3–C_4) (69)—α (C_1–C_2–C_3) (28)	α(ring)	a’	
24		420 (vs)	420 (ms)	405 (16.74, 04.65) 0.44	α (C_1–C_2–C_3) (60)—α(C_2–C_3–C_4)(26) + α(C_2–C_3–C_4)(4)—ν(N_2–C_3) (4)—β (C_1=O_{10}) (3)	α (ring)	a’	

Table 3 (continued)

S. No	Distribution of vibrational modes	Exp. recorded spectra (cm^{-1})		Theoretically calculated frequencies at the DFT/B3LYP/6–311 + + G**-09 level	PEDs	Assignments[$] for the characterizations of modes	Species	
		Figure 1(a)	Figure 2(a)					
		IR	Raman	5-chlorouracil	5-chlorouracil		In-plane	Out-of-plane
25		——-	410 (m)	382 (22.35, 00.69) 0.75	$\delta(C_2–C_3–C_4–C_5)$ (35)—$\delta(C_1–C_2–C_3–C_4)$ (27) + $\gamma(C_4–Cl_{12})$ (13) + $\gamma(N_8–H_9)$ (11)—$\gamma(C_5–H_6)$ (8) + $\gamma(C_3=O_{11})$ (4)	δ (ring)		a”
26		——	380 (m)	362 (06.36, 02.57) 0.36	$\alpha(C_2–C_3–C_4)$ (68) + α ($C_1–C_2–C_3$) (10)—$\nu(C_4–Cl_{12})$ (5) + $\beta(C_3=O_{11})$ (4)	β ($C_3=O_{11}$)	a’	
27			290 (s)	286 (00.44, 00.09) 0.75	$\gamma(C_4–Cl_{12})$ (36) + $\gamma(C_5–H_6)$ (26) -$\gamma(N_8–H_9)$ (20)—$\delta(C_3$-$C_4–C_5–H_6)$ (8) + $\delta(C_2–C_3–C_4–C_5)$(8)	γ ($C_5–Cl_{12}$)		a”

Table 3 (continued)

S. No	Distribution of vibrational modes	Exp. recorded spectra (cm^{-1})		Theoretically calculated frequencies at the DFT/B3LYP/6–311 + + G**-09 level	PEDs	Assignments[$] for the characterizations of modes	Species	
		Figure 1(a)	Figure 2(a)					
		IR	Raman	5-chlorouracil	5-chlorouracil		In-plane	Out-of-plane
28			260 (m)	227 (00.42, 01.08) 0.73	α (C_2–C_3–C_4) (49)—β(C_4 –Cl_{12}) (28) -α (C_1–C_2–C_3) (12) + β(C_3 = O_{11}) (4)	β (C_5 –Cl_{12})	a’	
29			240 (m)	143 (00.79, 00.01) 0.75	δ(C_3–C_4–C_5–H_6) (58)—δ(C_1–C_2–C_3–C_4) (35)—γ(N_2–H_7) (6)	δ (ring)		a”
30			200 (ms)	94 (01.33, 00.23) 0.75	δ (C_1–C_2–C_3–C_4) (64)—γ(N_8–H_9) (21) + δ (C_2–C_3–C_4-C_5)(7)	δ (ring)		a”

[#after the respective mode, in parentheses is % PED, but mode values < 3% are omitted of given Fig. 3 b.]

[*ν = very, w = weak, m = medium s = strong, sh = shoulder]

[$$\nu$ = stretching, α = angle bending, β = in-plane bending, γ = out-of-plane bending, δ = deformation.]

[+first and second values in parentheses show IR intensity (km/ mole) and Raman scattering activity ($\overset{0^4}{A}$ u^{-1}; as $\overset{0}{A} = 1 \times 10^{-10}$ m and 1u = 1 atomic mass unit = 1.6606×10^{-27} kg) but respective value above and below the parentheses shows the calculated frequency (in wave number $\equiv\nu$; cm^{-1}) and Raman band depolarization ratios.]

IR and at 1496 and 1425 cm^{-1} in Raman, respectively. In non-planar modes, the γ (N_2–H_7) and γ (N_8–H_9) modes have been optimized at 661 and 548 cm^{-1} and these have been recorded at 670 and 550 cm^{-1} in the IR and Raman at 670 and 555 cm^{-1}. Here, it is noticed that all of N–H stretching modes are much sensitive for the reason of the isolated in Ar matrix of molecule than the solid phase [19]. Here, it has been found that the above results are a similar agreement to the reported refs [9–21].

C=O (Six modes): The six C=O fundamental normal modes of 5-chlorouracil have been assigned as: $\nu(C_1{=}O_{10})$, $\nu(C_3{=}O_{11})$, $\beta(C_1{=}O_{10})$, $\beta(C_3{=}O_{11})$, $\gamma(C_1{=}O_{10})$ and $\gamma(C_3{=}O_{11})$. In case of uracil and their derivatives, the spectral region 1600–1800 cm^{-1} have been assigned with involving the congestion of carbonyl stretching modes and stretch mode of (C=C) bond [12–18]. These stretching modes have been affected with interaction of the H bonding and other important shifting modes for the reason of annoying of Fermi resonance [16–18]. Here, ν ($C_1{=}O_{10}$) and $\nu(C_3{=}O_{11})$ modes have been optimized at 1806 and 1776 cm^{-1} to respective modes, but the other mixing ring modes are given in the PEDs, and these have been recorded in the IR at 1792 and 1772 cm^{-1} with relating to Raman at 1810 and 1772 cm^{-1} of these modes and as the reported works [15–18]. In-plane, $\beta(C_1{=}O_{10})$ and $\beta(C_3{=}O_{11})$ bending modes have been optimized at 607 and 362 cm^{-1} and these have been recorded in IR at 610 and – cm^{-1}, but Raman bands at 630 and 380 cm^{-1} as reported in refs [12–18]. Non-planar modes $\gamma(C_1{=}O_{10})$ and $\gamma(C_3{=}O_{11})$ have been optimized at 749 and 764 cm^{-1}; similarly, these have been recorded at 750 and 760 cm^{-1} in IR, respectively, as well as at 750 and 760 cm^{-1} in Raman bands with strong intensities, but these have been mixed up with ring modes and H bonding.

In Ring modes (twelve modes): As phenyl ring, a pyrimidine ring of 5-chlorouracil has been assigned with the *12 fundamental modes*, namely the *6 stretching modes* in ring, *3 modes* in *deformation ring* in-plane and *3 modes* in *ring deformation* out-of-plane. These modes for stretching are complicated combination of C=C, C–N and C–C bonds in pyrimidine [15–18]. Here, because of spectral congestions of ν(C=O), some ring motions and H bonding modes, all stretching modes in ring have been found in the range of 1800–700 cm^{-1}. But, ν(C=C) vibration has been reported in the 1800–1600 cm^{-1} as assigned in the works [15–23]. Here, in the present work, 6 modes for ring stretching have been calculated at 1668 as $\nu(C_4{=}C_5)$, 1398, 1191, 1161 (Kekule), 970 and 776 cm^{-1}(ring breathing), and in order to the 1666, 1402, 1190, 1170, 960 and 775 cm^{-1} have been recorded in strong intensities for IR spectrum, consequently Raman bands at 1665, 1400, –, 1060, 930 and 776 cm^{-1} with the intensity of medium strong in observed results. Kekule (ν_{14} of benzene) mode of 5-chlorouracil [16] was calculated at 1163 cm^{-1}, but in this study, it is calculated to be lowered by 2 cm^{-1}. Now, the very popular ring breathing mode of 5-chlorouracil has been calculated at ~ 776 cm^{-1} which has lifted up to ~ 115 cm^{-1} than the 5-chlorouracil reported work of [16] at ~ 661 cm^{-1}, which is the modification for the above-reported result. For in-plane, the *3 modes* of ring deformation are calculated at 1075 (trigonal bending), 538 and 405 cm^{-1}; similarly, all of vibrations have been recorded in the IR at 1080, 540 and 420 cm^{-1} as well as the Raman bands at 1050, 535 and 420 cm^{-1} for the corresponding modes. In case of normal mode for trigonal bending

of 5-chlorouracil [16] was calculated at 971 cm^{-1} that has been found to be lowered by 104 cm^{-1} to the present result. But here, *three modes* for out-of-plane ring deformation are calculated at 382, 143 and 94 cm^{-1} and all of the calculated modes have been found to be almost similar to the reported work [16]. And so far, this could be found here that the above modes of ring deformation are correctly assigned in lower region possibly due to the PEDs.

Analysis of HOMO and LUMO

Molecular orbital's theory shows an important application for quantum studies of molecules to investigating the electronic level structure, optical and electrical properties [34]. The 5-chlorouracil bears 12 atoms and occupying with 74 electrons for 37 molecular orbitals (MOs), and the associated uracil molecule bears 12 atoms occupying with 58 electrons for the 29 molecular orbitals, whereas every molecular orbital (MO) has 2 electrons bearing the spins are stated as α (↑ spin) and β (↓ spin) like an opposite direction. Energy gap computation through HOMO–LUMO of 5-chlorouracil molecule has been done for the stability and reactivity. In study of HOMO and LUMO, energy levels of molecule advise a charge distribution probability as well as charge transfer in it. Energy gap levels suggest for this study about the active properties of molecule in the pharmacology.

The charge transfer properties of 5-chlorouracil have been studied with the help of the level energy analysis of HOMO and LUMO. For here, energy gap study supports for a charge transfer possibility properties in biomolecule. These have been studied for the stability and reactivity of *heterocyclic molecules* for the analysis of antiviral drugs against the new corona virus: COVID-19. Here, the *smaller energy gap* of 5-chlorouracil is more responsible to take place the charge transfer interaction in *heterocyclic drugs* that is the main reason of more bioactivity. The electron density mapping within electrostatic potential (MEP) plot and electrostatic potential (ESP) plotting within iso-surface plot have been evaluated in the next coming section for the charge distribution concepts in the molecule as the taking place of nucleophilic and electrophilic reactions.

Here, HOMO acts as electron donor, is limited at the bonds C–H, C–C, C–N and LUMO behaves as electron acceptor that is confined at location of bond C=C within ring. Thus, electronic transition of the HOMO to LUMO promotes from one part of ring bond (C=C) to other parts of pyrimidine bonds (C–N and C–C). In difference of energy level between HOMO and LUMO represents energy gap which evaluates reactivity and stability generally with lowest electronic energy level excitation of biomolecule. Therefore, electronic level transition corresponds through ground state to first excited level of state that this shows the excitation of electron from HOMO level to LUMO level. Here, it is possible that a smaller energy gap could be excited easily than higher energy gap. Hence, a smaller energy gap shows the reason for taking place of intracharge transformation in biomolecule as well as bioactivity. The larger energy band gap produces higher kinetic stability with that it shows the lower chemical reactivity; hence, this dislike for the addition of electrons to the higher lying LUMO but this removes the

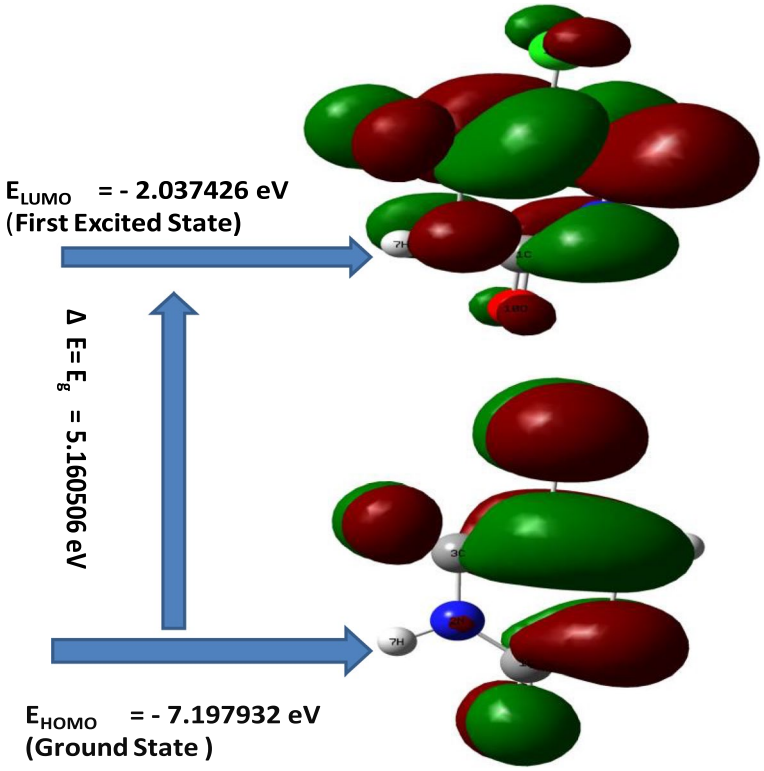

Fig. 4 Electronic energy levels with frontier MOs for 5-chlorouracil

Table 4 Lowest level energy value of HOMO and LUMO of 5-chlorouracil

Parameter	Energy (eV)
HOMO (for the ground level)	− 7.197932 eV
LUMO (for the first excited level)	− 2.037426 eV
HOMO–LUMO = the energy gap(Δ E)	**− 5.1605067 eV**

electrons from lower lying HOMO. Hence, for in any feasible reaction, the energy gap must be very small [35, 36]. Transition energy level of the HOMO to LUMO has been computed to be at **−5.1605067 eV** of 5-chlorouracil molecule. The transition through ground state to lowest excited level is the energy gap of molecule. In the energy gap, a frontier MOs from HOMO to LUMO produces the properties of chemical kinetic stability, polarizability, reactivity as well as hardness/softness of the biomolecule. The energy levels diagram with frontier figure of HOMO–LUMO of the 5-chlorouracil molecule is shown in Fig. 4. The energies of corresponding level as given in Table-4 of HOMO and LUMO are calculated as − 7.197932 eV and − 2.037426 eV represent a smallest energy of 5-chlorouracil. Therefore, energy gap between the MOs has been found to be − 5.1605067 eV in

5-chlorouracil molecule. Hence, this is clearly shown that a charge transfer (CT) happens within molecule. In energy gap, the ground level E_{HOMO} to first excited level E_{LUMO} is confirmed to show bioactivity as related to the intramolecular charge transfer (ICT) [37, 38].

After a successful trial of chloroquine for the treatment of COVID-19, the second one, 5-chlorouracil (**− 5.1605067 eV**) may be better antiviral drug than chloroquine after testing the clinical trial. These RNA-based constituent as antiviral drugs has shown promising results in clinical control of SARS-CoV-2 as molecular docking.

Analysis of molecular electrostatic potentials (MEPs)

In Fig. 5 (a), the surface plots of molecular electrostatic potentials have been shown for 5-chlorouracil biomolecule that is a most important computation generally used in the study of intermolecular characterization as well as the actions of drug molecule. In fact graphically, a spatial distribution of MEPs is represented as the chemical activities for a chemical reaction and strong binding on the active locations. MEP is directly connected with the chemical behavior, electronegativity and dipole moment of biomolecule. These plots are the visualization for the understanding of a relative polarity of that molecule and mappings their values in terms of electron densities (ED). MEPs surface plots have been traced with the help of the different colors as the given significance of electrostatic; red indicates the most -ve potential, blue indicates most + ve potential and green indicates zero potential regions in molecule. MEP increases as in sequence of colors: red, orange, yellow, green and blue on surface mapping/arrays. Here, negative MEP represents the attraction of a proton/light cation in the region of red color due to concentrated ED in the molecule, but the positive MEP represents the repulsion of the proton/cation in the region of blue color due to the atomic nuclei regions as the low concentration of ED in molecule. In Fig. 5 (a), red color represents -ve region and indicates the nucleophilic reactivity, but electrophilic reactivity is shown as blue for the positive region of surface plots of MEPs. As shown in Fig. 5 (a), the region of O_{11} atom is located with orange region, but the other O_{10} atom is located with the partially red area that this shows the electronegative area which is the place of nucleophilic reaction activity. On pyrimidine ring atoms, region of 3 H atoms is located with blue color as most positive region which is the active place of electrophilic attack. Here, green-colored location indicates zero potential. A shown in Fig. 5 (a) for MEP surface, this clearly indicates that the corner place of chloro group shows partially orange-colored region which has a negative electrostatic potential [Fig. 5 (a)].

The iso-surface plots for electrostatic potentials (ESPs) of 5-chlorouracil are shown in Fig. 5 (b), and the ESP explains the distribution of charge in molecule with the visualization for variable charged regions, so that charge distribution shows wide information that how a molecule acts and reacts with another molecule [39, 40]. ESPs are related to the electron density (ED) which explains as the reaction

Fig. 5 **a** Molecular electrostatic potentials (MEP) plot of 5-chlorouracil, **b** contour map plot of ESP iso-surface of 5-chlorouracil, **c** visualization for the mapping of total density of 5-chlorouracil, **d** visualization of the ESP array plot for 5-chlorouracil, **e** visualization of the total density array plot for 5-chlorouracil. ▶

locations of electrophilic effect and nucleophilic attacks and the H bonding interactions [41, 42].

As shown in Fig. 5 (b), the negative EPS shows the proton attraction due to the large electron density (given as red), and + ve EPS indicates for the proton repulsion where the small ED exists (shown as blue color). On iso-surface of ESP, the ED has a unified value, which is enclosed with the probability of specified fraction of electron density in molecule. In Fig. 5 (b), the ED has given with different coloring of iso-surface contours. At present, ESP has been shown in ascending through color order as: red, orange, yellow, green and blue. Such evaluate charge density, shape and chemical activity at the location. On iso-surface, the variation of ESPs values has been shown with variable colors as: red for the most -ve potential, blue for the most + ve potential and green for the zero electrostatic potential regions.

Representation of electrostatic potential for iso-surface has been graphically defined by Connolly [43–46] for a series of accessible surfaces. The electron density mapping for EPS iso-surface is shown in Fig. 5(b) of 5-chlorouracil. The mapping of total density as shown in Fig. 5 (c), the ESP array plot as shown in Fig. 5 (d) and total density array plot as shown in Fig. 5 (e) of 5-chlorouracil have been represented by the different colors. These diagrams of molecule have been visualized with chemically active location as well as comparative reactivity at atomic place. It could be seen in the region of Fig. 5 (d) and the neighborhood of atoms of pyrimidine ring of 5-chlorouracil, the yellow-colored lines stage as the region of electronegative these are found to be anywhere high closely or small closely that these behave as the nucleophilic or electrophilic attacks.

Analysis of thermodynamic functions

The three molecular motions such as vibrational, rotational and translational always contribute in the thermodynamic functions. In the DFT, the calculated wave numbers (in cm^{-1}) are applied to correct the properties of thermodynamic functional for 5-chlorouracil, and these are given in Table 5. In the computed theoretical thermodynamic data are applied for the correction of experimentally observed thermodynamic functions data at the temp zero Kelvin and an effect of zero-point vibrational energy (ZPVE). The scaling factors for the ZPVE has been applied somewhere for improving their overestimated data. The ZPVE and free energy have been calculated at − 874.482643 and − 874.515362 a.u. for the 5-chlorouracil, respectively. The calculated entropy of biomolecule could be applied in the correction of experimental data for thermodynamic information at the zero Kelvin temp to be caused to forget the residual entropy present at zero Kelvin temperature for crystalline phase. Through in computation, the entropies for translational, rotational and vibrational have been found to be at 40.846, 29.363

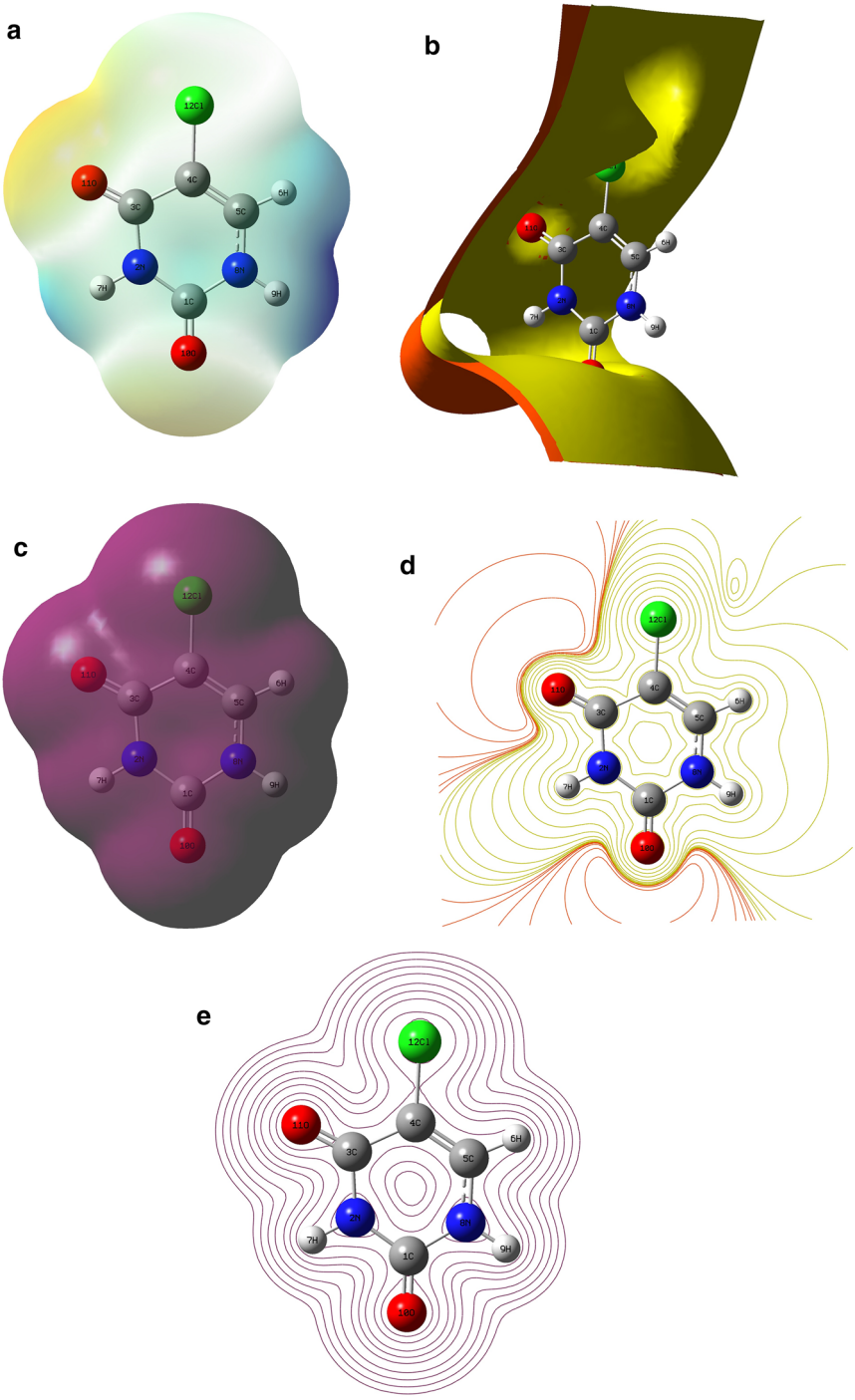
a
b
c
d
e
12Cl
11O
4C
3C
5C
6H
2N
8N
7H
1C
9H
10O

Table 5 Optimized thermodynamic functions (parameters) of 5-chlorouracil

Parameter	5-chlorouracil
(a)-Total energy and ZPE(AU)	− 874.482643
(b)-Gibb free energy (AU)	− 874.515362
©-Rotational constants (GHz):	3.04577
	0.98092
	0.74196
(d)-Entropy (Calmol^{-1} K^{-1}):	
Total:	86.502
(i)-Translational	40.846
(ii)-Rotational	29.363
(iii)-Vibrational	16.293
(e)-Dipole moments (Debyes)	4.1616

and 16.293 cal-mol^{-1} K^{-1} of 5-chlorouracil, respectively. Therefore, total entropy of the biomolecule is 86.502 cal-mol^{-1} K^{-1}, and the dipole moment is 4.1616 Debyes.

These above-computed thermodynamic parameters could be useful for the forth coming study to the related biomolecules. The computed results as given in Table 5 are helpful in an estimation of chemical reaction direction and some other thermodynamic energies of biomolecule. This study is worth mentioning that all these calculated parameters were done in the phase of gas state, but they could not be applied in the solution.

Conclusions

The all hydrogen atoms at pyrimidine ring in 5-chlorouracil are directly associated with nitrogen atoms bearing + ve Mulliken/APT charges. In all of the four C atoms (C_1, C_3, C_4, C_5), the C_4 atom has negative atomic polar tensor charge, but C_4 atom bears the positive Mulliken charge. Cl_{12} atom has the negative APT charges, but it bears the positive Mulliken charge. The computed geometrical parameters represent that all atoms in pyriminide as well as on ring's atoms are lying in a same plane.

All 30 vibrational fundamental modes have been assigned for chlorine atom mode with the help of experimental IR and Raman observation and calculated theoretical vibrational modes through G-09 as well as GAR2PED programs. In this study, Kekule (ν_{14}) mode of 5-chlorouracil has been observed at ~ 1161 cm^{-1} that is found to be lowered with 2 cm^{-1} and a popular ring breathing is at ~ 776 cm^{-1} that is shifted up to 115 cm^{-1} from the reported work [16] due to possible through the study of PEDs. In addition, the trigonal bending vibration of 5-chlorouracil is calculated at 1085 cm^{-1} that has been shifted up to 104 cm^{-1} in the present result and these some fundamental modes have been corrected for reported ref [16]. Here, the almost mixing modes to corresponding fundamental modes are given in PEDs.

In computation for HOMO–LUMO analysis, the energy gap are carried out with the suggested study for the charge distribution probability within biomolecule and in

the pharmacology. Here, the next one other drug, 5-chlorouracil, may be better antiviral drug than the chloroquine after testing the clinical trial. These RNA-based constituent as antiviral drugs has shown promising results in clinical control of COVID-19 as molecular docking. The MEPs and ESPs plots indicate around their locality of two O atoms have -ve potential and these are the active places for the nucleophilic attacks, and the chloro group atom has a –ve charge. And the locality of 3 H atoms at pyriminide is a place of most + ve as well as active region of electrophilic attack.

Acknowledgements Corresponding and first author is grateful to Prof. A. Pradhan, Department of Physics, I. I. T., Kanpur, for the needful help.

Funding No any funding source has supported for this work.

Declarations

Conflict of interest The authors declare that they have no conflict of interest.

References

1. Kirnos MD, Khudykov IY, Alexandrashikina NI, Vanyushin BF (1977) 2-Aminoadenine is an adenine substituting for a base in S-2L cyanophage DNA. Nature 270:369–370
2. Michel F, Hanna M, Green R, Bartel DP, Szostak JW (1989) The guanosine binding site of the *Tetrahymena* ribozyme. Nature 342:391–395
3. Person WB, Szczpaniak K (1993) Vibrational spectra and structure 20 Edited by J.R. Durig Chap 5:239–325
4. Farquharson S, Shendre C, Inscore FE, Paul Maksymiuk A, Gift, (2005) Analysis of 5 – fluorouracil in saliva using surface – enhanced Raman spectroscopy. J Raman Spectrosco 36:208–212
5. Graham MA, Lockwood GW, Greenslade D, Brienza S, Bayssas M, Gamelin E (2000) pharmacokinetics of oxaliplatin: a critical review. Clin Cancer Res 6:1205–1218
6. Nakajjma T (1995) Review of adjuvant chemotherapy for gastric cancer. Word J Surg 19:570–574
7. Billinghurst BE, Yeung R, Loppnow GR (2006) Excited-state structural dynamics of 5-fluorouracil. J Phys Chem A 110:6185–6191
8. Kim HO, Ahn SK, Alves AI, Beach IW (1992) Asymmetric synthesis of 1, 3-dioxolane-pyrimidine nucleosides and their anti-HIV activity. J Med Chem 35:1987–1995
9. Rastogi VK, Singh C, Vaibhav Jain M, Palafox A (2000) FTIR and FT-Raman spectra of 5-methyluracil (thymine). J Raman Spectrosco 31:1005–1012
10. Krishnakumar V, Ramasamy R (2007) Vibrational spectra and structure of 5, 6-diamino uracil and 5, 6-dihydro-5-methyl uracil by density functional theory calculations. Spectrochim Acta 66:503–511
11. Yarasi S, Billinghurst BE, Loppnow GR (2007) Vibrational properties of thymine, uracil and their isotopomers. J Raman Spectrosco 38:1117–1126
12. Alcolea Palafox M, Tardajos G, Guerrero-Martínez A, Rastogi VK, Mishra D, Ojha SP, Kiefer W (2007) FT-IR, FT-Raman spectra, density functional computations of the vibrational spectra and molecular geometry of biomolecule 5-aminouracil. Chem Phys 340:17–31
13. Rastogi VK, Palafox MA, Mittal L, Peica N, Kiefer W, Lang K, Ojha SP (2007) FTIR and FT-Raman spectra and density functional computations of the vibrational spectra, molecular geometry and atomic charges of the biomolecule: 5-Bromouracil. J Raman Spectrosco 38:1227–1241
14. Rastogi VK, Alcolea Palafox M, Guerrero-Martínez A, Tardajos G, Vats JK, I. Kostova¸S. Schlucker, W. Kiefer, (2010) FT-IR and FT-Raman spectra, ab initio and desity functional computations of the vibrational spectra, molecular geometry, atomic charges and some molecular properties of the biomolecule 5-iodouracil. J Mol Struct: THEOCHEM 940:29–44

15. Singh JS (2008) FTIR and Raman spectra comparing with ab initio calculated frequency modes for 5-aminouracil. J Mol Struct 876:127–133
16. Singh JS (2013) FT-IR and Raman Spectra, ab initio and density functional computations of the vibrational spectra, molecular geometries and atomic charges of uracil and 5-halogenated uracils (5-X-uracils; X= F, Cl, Br, I). Spectrochim. Acta A (G.B) 117:502–518
17. Singh JS (2014) IR and raman spectra, ab initio and density functional computations of the vibrational spectra, molecular geometries and atomic charges of uracil and 5-aminouracil. Spectrochim Acta A (GB) 130:313–328
18. Singh JS (2015) IR and Raman Spectra, ab initio and density functional computations of the vibrational spectra, molecular geometries and atomic charges of uracil and 5-methyluracil (thymine). Spectrochim. Acta A (GB) 137:625–640
19. Lapinski L, Nowak MJ, Bienkob DC, Michalska D (2002) Vibrational spectra of 5, 6-dihydrouracil. an experimental matrix isolation, solid state and theoretical study. Phys Chem Chem Phys 4:1123–1128
20. Barbara Morzyk-Ociepa and Danuta Michalska (2003) Vibrational spectra of 1-methyluracilate complex with silver (I) and theoretical studies of the 1-MeU anion. Spectrochim Acta A 59:1247–1254
21. Person WB, Szczepaniak K, Kwiatkowski JS (2002) Quantum mechanical and experimental infrared and Raman studies of 1-methyluracil and its hydrogen-bonded dimer. Int J Quantum Chem 90:995–1020
22. El'kin PM, Erman MA, Pulin OV (2006) Analysis of vibrational spectra of methyl-substituted uracils in the anharmonic approximation. J Appl Spectrosc 73(4):485–491
23. Choi MY, Miller RE (2007) Infrared laser spectroscopy of uracil and thymine in helium nanodroplets: vibrational transition moment angle study. J Phys Chem A 111:2475–2479
24. Frisch MJ et al (2010) Gaussian 09, Revision C.01,. G. Inc., Wallingford, CT
25. Dennington R II, Keith T, Millam J, GaussView, (2007) Version 412. Semichem Inc., Shawnee Mission, KS
26. Martin JMI, Van Alsenoy C (1995) GAR2PED. University of Antwerp, Belgium
27. Cioslowski J (1989) A new population analysis based on atomic polar tensors. JACS 111:8333–8336
28. Gussoni M (1986) Infrared intensities: a new tool in chemistry. J Mol Struct 141C:63–92
29. Person WB, Newton JH (1974) Dipole moment derivatives and infrared intensities. I Polar tensors J Chem Phys 61(3):1040–1049
30. Milano A, Castiglioni C (2010) Atomic charges from atomic polar tensors: a comparison of methods. J Mol Struct Theochem 955:158–164
31. Ferreira MMC, Suto E (1992) Atomic polar tensor transferability and atomic charges in the fluoromethane series CHxF4-x. J Phys Chem 96:8844–8849
32. Dewar MJS (1969) The molecular orbital theory of organic Chem. Mc. Graw- Hill and Inc., New York, USA
33. Coulson CA, McWeeny R (1979) Coulson's Valence. Oxford University Press, London
34. Pir H, Günay N, Avcı D, Atalay Y (2012) Molecular structure, vibrational spectra, NLO and NBO analysis of bis (8-oxy-1-methylquinolinium) hydroiodide. Spectrochim Acta A 96:916–924
35. Manolopoulos DE, May JC, Down SE (1991) Theoretical studies of the fullerenes: C_{34} to C_{70} Chem. Phys Lett 181:105–111
36. Dixit V, Yadav RA (2015) Experimental IR and Raman spectroscopy and DFT methods based material characterization and data analysis of 2- Nitrophenol. Biochem Pharmacol (Los Angel) 4:183–196
37. Padmaja L, Ravi Kumar C, Sajan D, Joe IH, Jayakumar VS, Pettit GR, Faurskov Nielsen O (2009) Density functional study on the structural conformations and intramolecular charge transfer from the vibrational spectra of the anticancer drug combretastatin-A2. J Raman Spectrosc 40:419–428
38. Sagdinc S, Pir H (2009) Experimental and ab initio computational studies on 4-(1H-benzo[d] imidazol-2-yl)-N, N-dimethylaniline. Spectrochim Acta A 73:181–194
39. Ozdemir N, Eren B, Dincer M, Bekdemir Y (2010) Experimental and ab initio computational studies on 4-(1H-benzo[d]imidazol-2-yl)-N. N-dimethylaniline Mol Phys 108:13–24
40. Politzer P, Murray JS (2002) The fundamental nature and role of the electrostatic potential in atoms and molecules. Theor Chem Acc 108:134–142

41. Luque FJ, Lopez JM, Orozco M (2000) Perspective on "Electrostatic interactions of a solute with a continuum a direct utilization of ab initio molecular potentials for the prevision of solvent effects." Theor Chem Acc 103:343–345
42. Okulik N, Jubert AH (2005) Theoretical analysis of the reactive sites of non-steroidal anti-inflammatory drugs. Int electron J Mol Des 4:17–30
43. Chattopadhyay B, Basu S, Chakraborty P, Choudhuri SK, Mukherjee AK, MonikaMukherjee, (2009) Synthesis, spectroscopic characterization, X-ray powder structure analysis, DFT study and in vitro anticancer activity of N-(2-methoxyphenyl)-3-methoxysalicylaldimine. J Mol Struct 932:90–96
44. Singh UC, Kollman PA (1984) An approach to computing electrostatic charges for molecules. J Comput Chem 5:129–145
45. Connolly ML (1983) Solvent-accessible surfaces of proteins and nucleic acids. Science 221:709–713
46. Muthu S, Maheswari U (2012) Quantum mechanical study and spectroscopic (FT-IR, FT-Raman, 13C, 1H, UV) study, first order hyperpolarizability, NBO analysis, HOMO and LUMO analysis of 4-[(4-aminobenzene) sulfonyl] aniline by ab initio HF and density functional method. Spectrochim Acta 92:154–163